Platinum-DNA adducts have recently been isolated by using enzymatic hydrolysis of the phosphodiester bond.[15-18] This method gives information about the base sequence of the DNA binding site which is lost by acid hydrolysis of the glycosyl linkage. However, the platinum-base adducts which are observed by the two methods can be compared. Both methods give similar results for the abundance of three types of platinum-base adducts and their kinetics of formation.

The initial fixation of *cis*-DDP on an oligonucleotide has recently been observed by X-ray crystallography.[30] The platinum atom binds to the N(7) position of Gua and, by means of a water bridge between the platinum and O(6), forms a seven-membered ring (N(7)-Pt-O-H-O(6)-C(6)-C(5)) which appears to destabilize the double helix of the DNA. After 2 h of reaction at 37 °C, this adduct accounts for about 10% of the recovered platinum. Apparently a majority of the monofunctional adduct reacts rapidly with DNA while about 10% disappears with a half-life of 24 h (Figure 2). These results show that the monofunctional adduct, *cis*-$[Pt(NH_3)_2(dGuo)(H_2O)]^{2+}$, chelates with DNA by two kinetically distinct reactions. The product of the first reaction is primarily a Gua_2 adduct. The product of the second reaction is preferentially, but not exclusively, *cis*-$[Pt(NH_3)_2(Gua)(Ade)]^{2+}$. Both reactions form Gua-Gua and Gua-Ade adducts and so the kinetic differences are probably not a consequence of different reactivity of the purine bases. Rather the monofunctional platinum-DNA adduct may react in two steps whose kinetics are determined by the relative positions of the bases at the binding site. A rapid reaction probably occurs with an adjacent purine base, preferably Gua. If an adjacent purine binding site is not available, a slower reaction may occur with a distant purine base.

Acknowledgment. We are grateful to Dr. R. C. Rao for measuring the NMR spectra and Sanofi Research for performing the elemental analysis. Financial assistance for this project was provided in part by grants from Federation Nationale des Centres de Lutte contre le Cancer, Federation Nationale des Groupements des Entreprises Françaises dans la Lutte contre le Cancer, and Sanofi Research.

Registry No. *cis*-DDP, 15663-27-1; *trans*-DDP, 14913-33-8; dGuo, 961-07-9; dAdo, 958-09-8; tu, 62-56-6; *cis*-$[Pt(NH_3)_2(dGuo)_2]Cl_2$, 98064-86-9; *trans*-$[Pt(NH_3)_2(dGuo)_2]Cl_2$, 98168-18-4; *cis*-$[PtCl(NH_3)_2(dGuo)]Cl$, 98064-87-0; *cis*-$[Pt(NH_3)_2(dGuo)(dAdo)]Cl_2$, 98087-59-3; *trans*-$[Pt(NH_3)_2(dGuo)(tu)_2]Cl_2$, 98064-88-1; *trans*-$[Pt(NH_3)(Guo)(tu)_2]Cl_2$, 98064-89-2; *cis*-$[Pt(NH_3)_2(Gua)_2]^{2+}$, 81628-84-4; *cis*-$[Pt(NH_3)_2(Gua)(Ade)]^{2+}$, 98064-91-6; *cis*-$[Pt(NH_3)_2(Gua)(H_2O)]^{2+}$, 98064-92-7; $[Pt(tu)_4]Cl_2$, 14552-88-6.

(30) Wing, R. M.; Pjura, P.; Drew, H. R.; Dickerson, R. E. *EMBO J.* **1984**, *3*, 1201-1206.

(31) Abbreviations used are as follows: DDP, $PtCl_2(NH_3)_2$; r_b, bound platinum per nucleotide; r_i, initial platinum per nucleotide; en, ethylenediamine; dien, diethylenetriamine; DDP-DNA, the complex formed between DDP and DNA; tu, thiourea.

Biosynthesis of Riboflavin. Incorporation of Multiply ^{13}C-Labeled Precursors into the Xylene Ring

Adelbert Bacher,[†] Quang Le Van,[†] Paul J. Keller,[‡] and Heinz G. Floss*[‡]

Contribution from the Lehrstuhl für Organische Chemie und Biochemie, Technische Universität München, D-8046 Garching, West Germany, and Department of Chemistry, The Ohio State University, Columbus, Ohio 43210. *Received April 12, 1985*

Abstract: The biosynthetic origin of the two 4-carbon units which give rise to the eight carbon atoms of the *o*-xylene moiety of riboflavin has been studied in stable isotope labeling experiments with cultures of the fungus *Ashbya gossypii*. Administration of precursors carrying multiple ^{13}C labels followed by NMR analysis of the enrichment and ^{13}C-^{13}C coupling patterns in the resulting riboflavin samples established unequivocally that each of the identical 4-carbon units arises from the intact carbon chain of a pentose derivative by an intramolecular rearrangement process involving excision of C4 and reconnection of C3 and C5.

Knowledge on the biosynthesis of riboflavin (**3**) has expanded considerably in recent years (Figure 1).[2,3] The first committed biosynthetic step consists of the opening of the imidazole ring of GTP by the enzyme GTP cyclohydrolase II.[4] Two subsequent enzymatic steps lead to the formation of 5-amino-6-(ribitylamino)-2,4-(1*H*,3*H*)-pyrimidinedione 5′-phosphate (**1**).[5-10] The conversion of this compound to 6,7-dimethyl-8-ribityllumazine (**2**) requires the addition of four carbon atoms, the origin of which is so far incompletely understood. A variety of potential precursors such as acetoin,[11,12] diacetyl,[13] pyruvate,[14] a tetrose,[15,16] a pentose,[17] and the ribityl moiety of 5-amino-6-(ribitylamino)-2,4-(1*H*,3*H*)-pyrimidinedione[18,19] have been discussed in the past. A detailed review of earlier work has been presented.[20]

Valuable evidence has been obtained by incorporation of isotopically labeled precursors, which is conveniently studied at the biosynthetic level of riboflavin rather than 6,7-dimethyl-8-ribityllumazine.[1,17,20-24] Since the formation of riboflavin by a dismutation of **2** is well understood,[25-27] the labeling pattern of the latter compound can be easily inferred from the distribution

[†] Technische Universität München.
[‡] The Ohio State University.

(1) (a) Floss, H. G.; Le Van, Q.; Keller, P. J.; Bacher, A. *J. Am. Chem. Soc.* **1983**, *105*, 2493-2494. (b) Keller, P. J.; Le Van, Q.; Bacher, A.; Kozlowski, J. F.; Floss, H. G. *J. Am. Chem. Soc.* **1983**, *105*, 2505-2507.
(2) Plaut, G. W. E. In "Comprehensive Biochemistry"; Florkin, M., Stotz, E. H., Eds.; Elsevier: Amsterdam, 1971; Vol. 21, pp 11-45.
(3) Plaut, G. W. E.; Smith, C. M.; Alworth, W. L. *Annu. Rev. Biochem.* **1974**, *43*, 899-922.
(4) Foor, F.; Brown, G. M. *J. Biol. Chem.* **1975**, *250*, 3545-3551.
(5) Lingens, F.; Oltmanns, O.; Bacher, A. *Z. Naturforsch.* **1967**, *22B*, 755-758.
(6) Burrows, R. B.; Brown, G. M. *J. Bacteriol.* **1978**, *136*, 657-667.
(7) Hollander, I.; Brown, G. M. *Biochem. Biophys. Res. Commun.* **1979**, *89*, 759-763.
(8) Logvinenko, E. M.; Shavlovskii, G. M.; Zakal'skii, A. E.; Senyuta, E. *Z. Biokhimiya* **1980**, *45*, 1284-1292.
(9) Klein, G.; Bacher, A. *Z. Naturforsch.* **1980**, *35B*, 482-484.
(10) Nielsen, P.; Bacher, A. *Biochim. Biophys. Acta* **1981**, *662*, 312-317.
(11) Goodwin, T. W.; Treble, D. H. *Biochem. J.* **1958**, *70*, 14P-15P.
(12) Kishi, T.; Asai, M.; Masuda, T.; Kuwada, S. *Chem. Pharm. Bull. (Tokyo)* **1959**, *7*, 515-519.

0002-7863/85/1507-6380$01.50/0

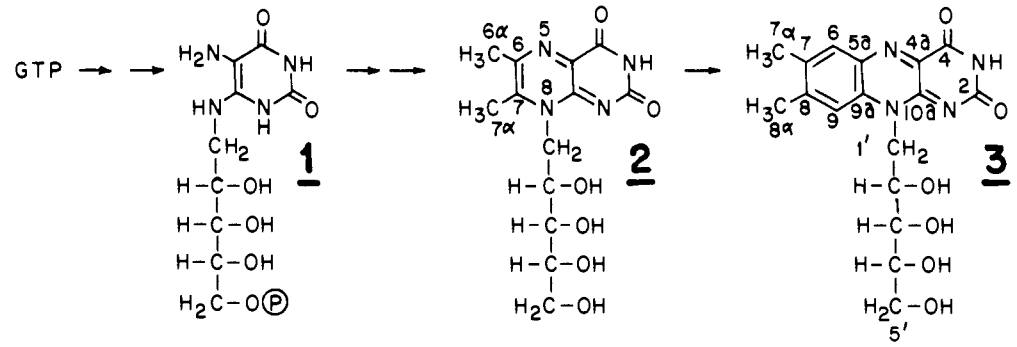

Figure 1. Biosynthesis of riboflavin.

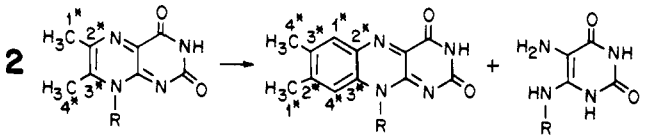

Figure 2. Regiochemistry of riboflavin synthase. Numbers with asterisks indicate an arbitrary nomenclature.

of isotope in the final product, riboflavin. We found it advantageous to disignate the carbon atoms of the hypothetical 4-carbon unit (4C-unit), which is required for the formation of the pyrazine ring of **2**, by consecutive numbers 1*–4* (Figure 2). Given the regiospecificity of riboflavin synthase as described by Beach and Plaut,[27] 1* corresponds to C6α of the lumazine and to C6 and C8α of riboflavin.

It was recognized early that isotope incorporation studies directed at the biosynthesis of the xylene ring could benefit from a comparison of the incorporation patterns into the 4C-unit and the ribityl side chain of riboflavin.[21,22] The origin of the ribityl moiety from the ribose moiety of GTP is well established.[28] It follows that the side chain provides comprehensive information on the labeling pattern of the pentose pool. The labeling pattern of other carbohydrate pools can also be partially inferred from these data.[20]

Early work of Plaut and Broberg has shown that acetate is not a direct precursor of the xylene ring.[21,22] It was also shown that both C1 and C6 of hexoses could contribute with comparable efficiency to the labeling of 1* and/or 4* of the 4C-unit. However, due to the pseudosymmetry of the xylene ring, 1* could not be distinguished from 4*, and 2* could not be distinguished from 3*.

The advent of ^{13}C NMR techniques permitted unequivocal determination of enrichments for each carbon atom in the analysis of biosynthetic ^{13}C-labeling experiments. We were able to show a close correlation between the enrichments of the carbon atoms 1* through 3* with C1 through C3 of the pentose pool.[20,23] However, C4* paradoxically appeared to correspond to C5 of the pentose pool and C4 of pentoses had no equivalent in the xylene ring. This finding could be due either to fortuitous correspondence or formation of the 4C-unit from a pentose through a skeletal rearrangement with elimination of the pentose C4.

In the present work we have examined the correlation of carbon–carbon bonds in the pentose pool, as monitored by the ribityl moiety of **3**, with those of the 4C-unit. The correlation of bonds, i.e., contiguous intact incorporation of two or more carbon atoms, intrinsically provides stronger biochemical evidence than the equivalent study of individual atoms. To this end, biosynthetic feeding experiments using multiply ^{13}C-labeled precursors were undertaken. Some of the results have been communicated in preliminary form.[1]

Experimental Section

Materials. The following compounds were obtained from commercial sources: [1,2-$^{13}C_2$]acetate from Prochem, London, England; [U-$^{13}C_6$]-glucose and [1,3-$^{13}C_2$]glycerol from MSD, St. Louis, Missouri; [1,3-$^{13}C_2$]ribose and [2,3-$^{13}C_2$]ribose from Omicron Biochemicals, Ithaca, New York. [2,3-$^{13}C_2$]Succinate was synthesized by published standard procedures.[29]

Organism and Fermentation. *Ashbya gossypii* ATCC 10895 was used for all the investigations mentioned herein. Maintenance of the culture, fermentations, and ^{13}C-labeling experiments were carried out as previously described.[20] Fermentation was continued for 12 or 24 h after addition of a labeled precursor. The culture fluid was separated from the mycelium by filtration. The mycelium was washed with 400 mL of 20% acetic acid. The culture fluid and the washing fluid were combined and lyophilized.

Extraction and Purification of Riboflavin. An improved isolation procedure was developed. The residue obtained by lyophilization of the culture medium and washing fluid was dissolved in 100 mL of deionized water. The aqueous solution was extracted four times with 100 mL of benzyl alcohol for about 1 h. The resulting emulsions were broken by centrifugation (4 °C, 12000 rpm, 1 h). The benzyl alcohol extracts were pooled, diluted with 3 volumes of diethyl ether, and extracted twice with 100 mL of deionized water. The aqueous solution was washed twice with 600 mL of diethyl ether and evaporated to dryness under reduced pressure. The crude riboflavin residue was triturated with dichloromethane (50 mL) in order to dissolve residual benzyl alcohol. Diethyl ether (200 mL) was added to the suspension, and the mixture was allowed to stand for 2 h. The supernatant was decanted and discarded. This procedure was repeated twice. Finally the riboflavin residue was dissolved in 500 mL of deionized water and applied to a column of AG 50 WX8 (H^+ form, 200–400 mesh, 2.3 × 40 cm). The column was developed with 0.1 M HCl. Fractions were combined and evaporated to dryness under reduced pressure.

Acetylation of Riboflavin. Riboflavin was acetylated as described earlier.[20] The residue obtained after chromatography on silica gel was dissolved in about 20 mL of dichloromethane. Aliquots of 1 mL were subjected to high-performance liquid chromatography on a column of Lichrosorb Si 60 (7 um, 3 × 250 mm) from Merck AG, Darmstadt, West Germany. The column was developed with 1% methanol in dichloromethane. The flow rate was 1 mL/min. The retention time of riboflavin

(13) Bryn, K.; Stormer, F. C. *Biochim. Biophys. Acta* **1976**, *428*, 257–259.
(14) Katagiri, H.; Takeda, I.; Imai, K. *J. Vitaminol. (Kyoto)* **1959**, *5*, 287–297.
(15) Alworth, W. L.; Baker, H. N.; Winkler, M. F.; Keenan, A. M.; Gokel, G. W.; Wood, F. L. *Biochem. Biophys. Res. Commun.* **1970**, *40*, 1026–1031.
(16) Ali, S. N.; Al-Khalidi, U. A. S. *Biochem. J.* **1966**, *98*, 182–188.
(17) Alworth, W. L.; Dove, M. F.; Baker, H. N. *Biochemistry* **1977**, *16*, 526–631.
(18) Bresler, S. E.; Perumov, D. A.; Chernik, T. P.; Glazunov, E. A. *Genetika* **1976**, *12*, 83–91.
(19) Hollander, I. J.; Braman, J. C.; Brown, G. M. *Biochem. Biophys. Res. Commun.* **1980**, *94*, 515–521.
(20) Bacher, A.; Le Van, Q.; Keller, P. J.; Floss, H. G. *J. Biol. Chem.* **1983**, *258*, 13431–13437.
(21) Plaut, G. W. E. *J. Biol. Chem.* **1954**, *211*, 111–116.
(22) Plaut, G. W. E.; Broberg, P. L. *J. Biol. Chem.* **1956**, *218*, 131–138.
(23) Bacher, A.; Le Van, Q.; Bühler, M.; Keller, P. J.; Eimicke, V.; Floss, H. G. *J. Am. Chem. Soc.* **1982**, *104*, 3754–3755.
(24) Keller, P. J.; Le Van, Q.; Bacher, A.; Floss, H. G. *Tetrahedron* **1983**, *29*, 3471–3481.
(25) Plaut, G. W. E. *J. Biol. Chem.* **1963**, *238*, 2225–2243.
(26) Wacker, H.; Harvey, R. A.; Winestock, C. H.; Plaut, G. W. E. *J. Biol. Chem.* **1963**, *239*, 3493–3497.
(27) Beach, R. L.; Plaut, G. W. E. *J. Am. Chem. Soc.* **1970**, *92*, 2913–2916.
(28) Mailänder, B.; Bacher, A. *J. Biol. Chem.* **1976**, *251*, 3623–3628.
(29) Renaud, R. N.; Leitch, L. C. *J. Labelled Compd.* **1973**, *9*, 145–158.

tetraacetate was 28 min. Elution was monitored photometrically (254 nm). Fractions were collected and evaporated to dryness under reduced pressure.

^{13}C NMR Spectroscopy. ^{13}C NMR spectra were measured at 50.3 MHz (4.7 T) on a Bruker WP-200 FT-NMR spectrometer or at 75.4 MHz (7.0 T) on a Bruker WM-300 FT-NMR spectrometer. Samples were dissolved in $CDCl_3$ with or without 0.1 M $Cr(AcAc)_3$[30] (Sigma, recrystallized from hot methanol before use). For samples without $Cr(AcAc)_3$ the measured conditions were the following: 60° pulse, repetition time = 2.0 s, spectral width = 11.11 kHz (15.15 kHz for WM-300 measurements), 32K data sets, 0.5 Hz line broadening, continuous broadband ^{1}H decoupling. For samples with $Cr(AcAc)_3$ the conditions were the following: 90° pulse, repetition time = 1.2 s, spectral width = 11.11 kHz (15.15 kHz for WM-300), 16K data set zero-filled to 32K, 1.0 Hz line broadening, inverse gated broadband ^{1}H decoupling (i.e., decoupler on only during data acquisition). Spectra of natural abundance riboflavin tetraacetate acquired with $Cr(AcAc)_3$ showed that the integrals of all the signals were equal with ±6.5%. Inversion–recovery T_1 relaxation measurements showed that the longest T_1 under these conditions was 0.5 s.

Relative ^{13}C enrichment values were calculated as follows. From spectra of natural abundance riboflavin tetraacetate with and without $Cr(AcAc)_3$, the average of the integrals over the acetate methyl or carbonyl signals was assigned a value of 1 unit, and all other signal integrals were standardized to this scale. The same procedure was followed for the labeled samples. Relative enrichments were calculated as the ratios of the standardized integrals for the labeled sample vs. the natural abundance sample.

When necessary, a simple line shape deconvolution routine was used to obtain integrals for partially overlapped signals. Spin calculations (PANIC program from Bruker) for AB and ABC spin systems were used to calculate the intensities of portions of multiplets which were overlapped by other signals.

Results and Discussion

The described fermentation and isolation procedures typically yielded ca. 40 mg of riboflavin from 200 mL of culture fluid. This material was chemically converted into the 2′,3′,4′,5′-tetraacetate derivative prior to NMR analysis. The tetraacetate has the advantages of solubility and of providing a ^{13}C natural abundance standard in the form of NMR signals from the acetate residues. The ^{13}C NMR assignments for riboflavin tetraacetate in chloroform have been unambiguously determined by selective labeling, T_1 measurements, and 2D- and multiple quantum NMR studies.[20,24] When viewing the data from the present experiments, it is necessary to bear in mind the presence of a large excess of unlabeled glucose in the fermentation media.

The ^{13}C enrichments and the amount of ^{13}C–^{13}C coupling at each carbon site were determined for each of the riboflavin tetraacetate samples. In some cases, for example C9, it was not possible to separate coupling contributions from the two neighboring carbon atoms (C9a and C8) since both couplings are first order and of approximately equal magnitude.

As described earlier, the presence of a neighboring ^{13}C can affect the relaxation (and thus also the NOE) of an observed ^{13}C.[24] This effect, as expected, was found to be significant only for nonprotonated observed carbon sites, and especially for C5a and C9a which exhibit the longest T_1 relaxation times in the xylene ring. Thus, it was necessary to make two ^{13}C NMR measurements of each sample displaying significant one-bond ^{13}C–^{13}C coupling: one measurement employing the usual broadband ^{1}H decoupling and the other after the addition of the electronic relaxation agent $Cr(AcAc)_3$ and with use of an inverse gated ^{1}H-decoupling scheme. The latter technique permitted the measurement of the quaternary carbons in the absence of the relaxation effects of neighboring ^{13}C nuclei.

It was desirable to obtain a semiquantitative measure of the intact incorporation of doubly labeled precursors into biosynthetic product. A numerical treatment of ^{13}C–^{13}C coupling data was devised, the details of which will be published elsewhere.[31] A static model for biosynthetic incorporation is used in conjunction

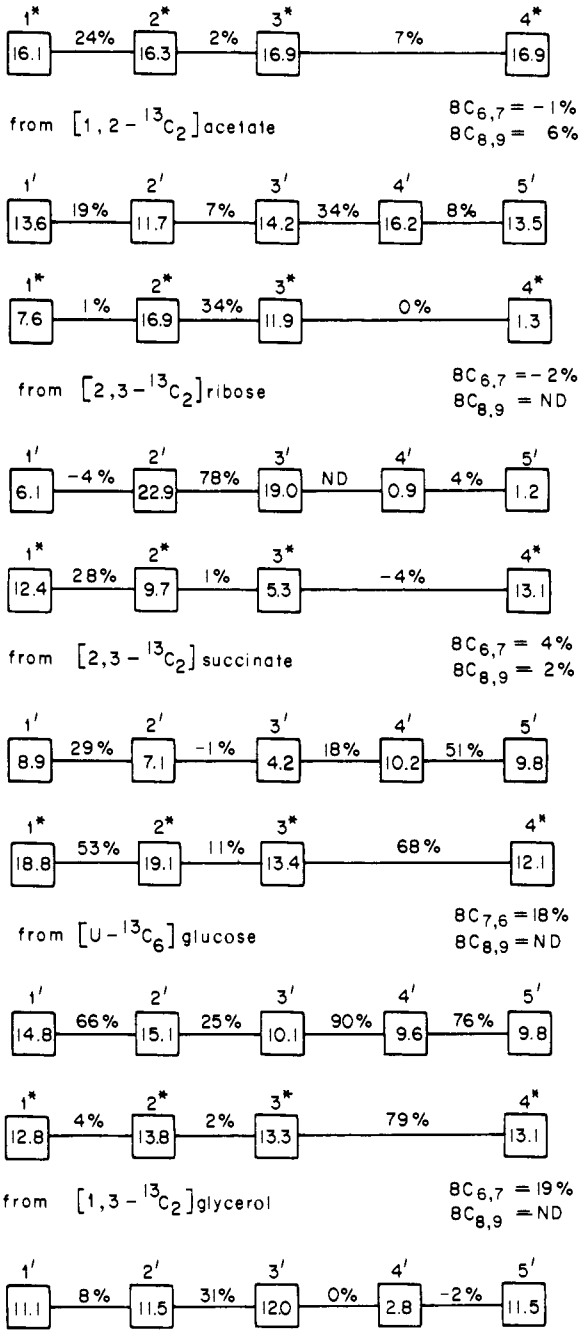

Figure 3. ^{13}C enrichments and BC values for riboflavin tetraacetate derived by fermentation from the precursors indicated.

with observed values for amounts of coupling and enrichments to obtain a quantity denoted as BC. BC (for biochemical connectivity) is the percentage of the total amount of ^{13}C in two neighboring product carbon atoms which is due to intact incorporation of a doubly ^{13}C-labeled precursor. This treatment allows distinction between coupling from intact incorporation and coupling due to statistical recombination of ^{13}C-atoms arising from general enrichment of metabolic carbon pools. There are many possible sources of error in this analysis, not the least of which is that this is a static interpretation of a dynamic system. However, there exist reference points in the system. For example, the bonds between the two 4C-units in the xylene ring and in some cases the C2′–C3′ bond in the side chain should not show biochemical connectivity.

The following precursors were fed to the fungus: [1,2-$^{13}C_2$]-acetate (17 mM, 12 h fermentation after addition of label); [2,3-$^{13}C_2$]succinate (5.7 mM, 12 h); [U-$^{13}C_6$]glucose (6.5 mM, 24 h); [2,3-$^{13}C_2$]ribose (7.8 mM, 24 h); [1,3-$^{13}C_2$]ribose (7.8 mM, 24 h); [1,3-$^{13}C_2$]glycerol (9.8 mM, 24 h). The resulting enrich-

(30) Abbreviation used: $Cr(AcAc)_3$, chromium(III) acetoacetonate.
(31) (a) Keller, P. J.; Bown, D. H., unpublished results. (b) London, R. E.; Kollman, V. H.; Matwiyoff, N. A., *J. Am. Chem. Soc.*, **1975**, *97*, 3565–3573.

Table I. Relative ^{13}C Enrichments of Riboflavin Tetraacetate from the Precrusors Indicated[a]

carbon	ppm	[1,2-$^{13}C_2$]acetate	[2,3-$^{13}C_2$]succinate	[1,3-$^{13}C_2$]glycerol	[2,3-$^{13}C_2$]ribose	[1,3-$^{13}C_2$]ribose[b]
2	154.6	9.2	5.2	2.1	1.3	1.2
4	159.3	6.1	2.4	2.5	1.6	1.3
4a	136.0	7.6	1.5	1.0	1.3	1.1
5a(2*)	134.5	17.1	10.4	14.5	17.3	7.1
6(1*)	132.8	17.2	13.0	13.7	7.6	11.6
7(3*)	136.9	17.1	5.2	13.6	12.1	12.0
7α(4*)	19.4	17.2	13.3	13.5	1.2	1.1
8(2*)	148.0	15.6	8.9	13.1	16.5	7.0
8α(1*)	21.4	14.9	11.7	11.9	7.5	11.1
9(4*)	115.5	16.6	12.9	12.6	1.3	1.2
9a(3*)	131.1	16.7	5.4	12.9	11.7	11.9
10a	150.6	2.1	1.1	1.2	1.2	1.0
1′	44.9	13.6	8.9	11.1	6.1	18.1
2′	69.3	11.7	7.1	11.5	22.9	5.3
3′	70.4	14.2	4.2	12.0	19.0	18.7
4′	68.9	16.2	10.2	2.8	0.9	1.2
5′	61.8	13.5	9.8	11.5	1.2	1.1
CH_3CO[c]	ca.170	1.0[d]	1.0[d]	1.0[d]	1.0	1.1
CH_3CO[c]	ca. 21	1.3	1.2	1.2	1.0[d]	1.0[d]

[a] Enrichments of carbon atoms in the isoalloxazine ring system were determined with samples containing $Cr(AcAc)_3$, while side chain enrichments were measured for sample without added $Cr(AcAc)_3$. Chemical shifts were determined in $CDCl_3$ and are referenced to Me_4Si. [b] All enrichments determined without $Cr(AcAc)_3$. [c] Average of four signals. [d] Natural abundance standard.

Table II. Amounts of ^{13}C–^{13}C Coupling of Riboflavin Tetraacetate Samples Obtained from the Precursors Indicated

	J(partner)									
	coupling		[1,2-$^{13}C_2$]acetate		[2,3-$^{13}C_2$]succinate		[1,3-$^{13}C_2$]glycerol		[2,3-$^{13}C_2$]ribose	
obsd carbon	partner	*J*, Hz	% coupling[a]	BC, %	% coupling	BC, %	% coupling	BC, %	% coupling	BC, %
4	4a	77	NO	ND	NO	ND	NO	ND	NO	ND
4a	4	77	NO	ND	NO	ND	NO	ND	NO	ND
4a	10a	53	ND	47	NO	ND	ND	ND	NO	ND
5a	6	69	31	25	38	27	24	5	12	3
5a	9a	59	21	0	4	−1	14	6	27	32
6	5a	69	37	25	26	27	14	5	16	3
6	7	60	20	−1	8	4	27	19	15	−2
7	6	60	17	−1	13	4	28	19	5	−2
7	7α	44	29	13	7	−5	71	82	1	0
7	8	53	16	3	8	3	14	−1	45	37
7α	7	44	24	13	4	−5	76	82	13	0
8	7	53	24	3	10	3	15	−1	35	37
8	8α	43	30	22	36	28	16	4	6	−2
8	9	62	22	6	16	2	ND	ND	ND	ND
8α	8	43	31	22	27	28	17	4	20	−2
9	8	62	20	6	11	2	ND	ND	ND	ND
9	9a	66	19	1	5	−2	70	76	ND	ND
9a	9	66	19	1	12	−2	68	76	ND	ND
9a	5a	59	16	0	14	−1	24	6	49	32
10a	4a	53	33	47	NO	ND	NO	ND	NO	ND
1′	2′	41	26	19	24	29	16	8	20	−4
2′	1′	41	27	19	38	29	20	8	5	−4
2′	3′	44	13	7	4	−1	34	31	74	78
3′	2′	44	18	7	6	−1	34	31	68	78
3′	4′	46	40	34	35	18	3	0	ND	ND
4′	3′	46	37	34	14	18	15	0	ND	ND
4′	5′	42	15	8	47	51	9	−2	5	4
5′	4′	42	29	8	50	51	2	−2	5	4

[a] Calculated as the percentage of the total ^{13}C NMR signal for a given carbon atom which is due to coupling with a specified neighbor. NO = not observed, ND = not determined.

ment and coupling data are given in Tables I and II, respectively. None of the data for the incorporation of label into the side chain are in conflict with known pentose metabolic pathways as previously discussed.[20,24] We attempt to examine several aspects of the data set in a search for both positive and negative evidence concerning the formal relationship of the 4C-unit with the pentose pool.

Examination of the enrichment data is facilitated by the box schemes presented in Figure 3, where numbers in the boxes represent relative ^{13}C enrichments for the indicated site. Numbers between the boxes are the BC values, indicating the extent of intact incorporation. Averages of the two values for the biogenetically equivalent sites of the 4C-unit are given. In each case, high or low enrichment of C1′ is echoed in C1*. The same is also true for the relationships of C2′ with C2*, C3′ with C3*, and C5′ with C4*, while the enrichment pattern of C4′ is not reflected in the 4C-unit. This is in accord with our earlier work with single ^{13}C labels.[20]

Diagrammatic overviews of the coupling data are shown in Figures 3 and 4. Significant biochemical connectivity was detected for the C1′–C2′ bond of riboflavin tetraacetate samples from [U-$^{13}C_6$]glucose, [2,3-$^{13}C_2$]succinate, and [1,2-$^{13}C_2$]acetate. Although neither acetate nor succinate are direct precursors of the 4C-unit, these labeled compounds as well as the glucose yielded couplings for C1*–C2* of the 4C-unit. This is taken as evidence of the correspondence of the C1*–C2* bond with the C1–C2 bond of a pentose. The samples derived from [2,3-$^{13}C_2$]ribose and [1,3-$^{13}C_2$]glycerol further support this correlation with negative evidence; these samples displayed neither C1′–C2′ connectivity nor C1*–C2* connectivity. However, the glycerol experiment does not yield entirely clear evidence for this bond for reasons discussed below.

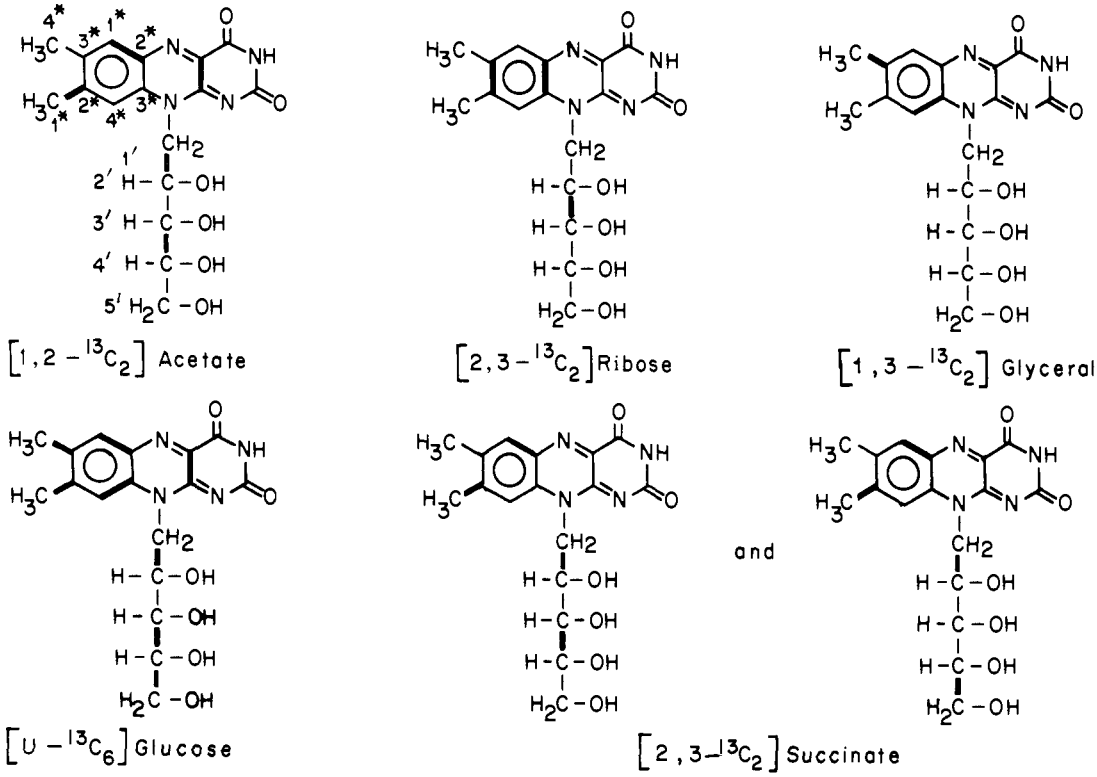

Figure 4. Schematic representation of contiguously transferred neighboring carbons.

Coupling for the C2′–C3′ bond was observed with riboflavin derived from [2,3-$^{13}C_2$]ribose and [1,3-$^{13}C_2$]glycerol. In general it was difficult to obtain reliable information on this bond. If pentoses originate from trioses or citric acid cycle intermediates (e.g., in experiments with acetate, succinate, and glycerol), the C2–C3 bond is formed de novo. Hence no coupling transfer should be expected. Starting from a labeled hexose does not improve the situation. Conversion to pentose phosphate through the pentose phosphate cycle involves breaking of the C2–C3 and the C3–C4 bonds of the proffered hexose. In addition, the latter bond is easily broken by futile glycolytic shuttling.[32] In light of this, it is not surprising that only the sample from [2,3-$^{13}C_2$]ribose yielded high biochemical connectivity for C2′–C3′. The coincident coupling of C2*–C3* established a correlation between these two bonds. The existence of significant coupling for C2′–C3′ for the glycerol sample probably reflects efficient uptake of this intermediate leading to relatively high labeling of the triose pool soon after addition of the precursor. This flooding of the triose pool, in turn, yields a significant amount of [1,3,4,6-$^{13}C_4$]hexose, giving rise to the observed C2–C3 coupling in the pentose pool. The significance of this kinetic effect in regard to the correlation of pentoses with the 4C-unit is uncertain.

The correlation of the three-carbon segment C1–C2–C3 of a pentose with C1*–C2*–C3* was obtained from the experiment with [1,3-$^{13}C_2$]ribose. The product riboflavin showed two-bond long-range couplings for C1′–C3′, C6–C9a (1*–3*) (Figure 5), and to a lesser extent C8α–C7 (1*–3*) for which the coupling constant is smaller.

Biochemically significant couplings for C3′–C4′ were observed for samples derived from [U-$^{13}C_6$]glucose, [1,2-$^{13}C_2$]acetate, and [2,3-$^{13}C_2$]succinate. However, of these samples only the riboflavin from [U-$^{13}C_6$]glucose yielded 3*–4* coupling. This information must be considered in conjunction with that for the C4′–C5′ bond, which displayed coupling only in samples from [U-$^{13}C_6$]glucose and [2,3-$^{13}C_2$]succinate. The succinate and glucose samples are complementary in that the sample from succinate gave coupling C3′–C4′ and C4′–C5′ in separate molecules. In contrast, the glucose derived riboflavin displayed coupling C3′–C4′–C5′ in the same molecule, i.e., C4′ was doubly coupled. The only way to reconcile the observations for these two samples is to propose an intramolecular rearrangement in which C3 and C5 of a pentose are joined with concomitant excision of the pentose C4. This conclusion is supported by the single ^{13}C-labeling experiments, which indicate the non-incorporation of C4 of a pentose into the 4C-unit, as well as similar results from in vitro ^{14}C-labeling experiments.[20,33]

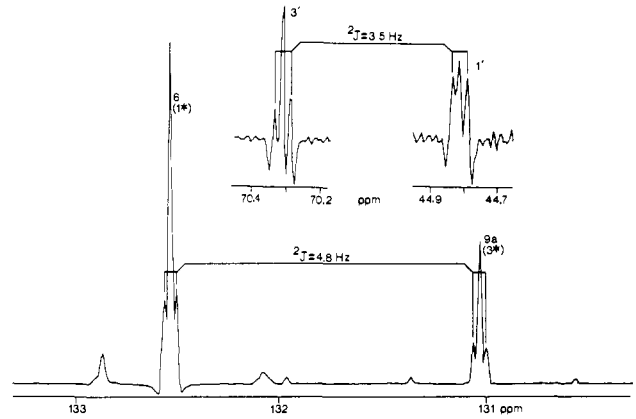

Figure 5. Portions of the ^{13}C NMR spectrum of riboflavin tetraacetate from [1,3-$^{13}C_2$]ribose. Intensities of signals in different traces cannot be directly compared due to the differing degrees of resolution enhancement.

More direct confirmation of this rearrangement was clearly desirable, which was the rationale for an incorporation experiment utilizing [1,3-$^{13}C_2$]glycerol. No one-bond coupling was observed for either C3′–C4′ or C4′–C5′. In the 4C-unit, up to 75% of the C3* and C4* signals were in the one-bond coupling satellites, yielding BC values of 81% and 76% for C3*–C4*. This is taken as unequivocal confirmation of the proposed rearrangement.

The sum of the data presented here along with those reported earlier[20,24] are all in accord with the notion that the 4C-unit of riboflavin is derived from pentose metabolism via an intramolecular

(32) Sillerwood, L. O.; Shulman, R. G. *Biochemistry* **1983**, *22*, 1087–1094.

(33) Nielsen, P.; Neuberger, G.; Floss, H. G.; Bacher, A. *Biochem. Biophys. Res. Commun.* **1984**, *118*, 814–822.

rearrangement in which C4 of a pentose is excised and C3 and C5 are reconnected intramolecularly. The data offer no information concerning whether the more proximal precursor is a pentose or a pentulose, nor is it possible to draw conclusions about which pentose/pentulose stereoisomer (e.g., ribose, xylose, etc.) is employed in this intriguing biosynthesis. Labeling experiments in vitro are under way to investigate the nature of intermediates in this pathway.

Acknowledgment. We thank Dr. H. Otsuka, now at Hiroshima University, Japan, for the preparation of [2,3-$^{13}C_2$]succinate and Angelika Kohnle and Kay Kampsen for secretarial assistance. We also thank Dr. David H. Bown for helpful discussions. Financial support is acknowledged from the Deutsche Forschungsgemeinschaft and the Fonds der Chemischen Industrie (grants to A.B.), the National Institutes of Health (grant to P.J.K. and H.G.F.), and the Alexander von Humboldt Foundation (fellowship to P.J.K. and Senior US Scientist Award to H.G.F.).

Registry No. *o*-MeC_6H_4Me, 95-47-6; riboflavin, 83-88-5; acetate, 64-19-7; ribose, 50-69-1; glycerol, 56-81-5; glucose, 50-99-7; succinate, 110-15-6.

Gold Carbonyl, Au(CO): Matrix Isolation ESR Study

Paul H. Kasai* and Paul M. Jones

Contribution from IBM Instruments, Inc., Orchard Park, Danbury, Connecticut 06810.
Received April 12, 1985

Abstract: ESR spectra of gold(0) monocarbonyl generated in argon matrices by cocondensation of gold atoms and CO molecules were observed and analyzed. The **g** tensor and the ^{197}Au and ^{13}C hyperfine-coupling tensors of the complex were determined. Also seen in the spectra were effects of the Au nuclear quadrupole moment; the effects were demonstrated, and the nuclear quadrupole coupling tensor was determined. It is shown that the complex is formed by the dative interaction of the lone-pair electrons of CO with a vacant sp_σ orbital of the metal atom and the back-donation from the metal d_π orbitals into the antibonding π^* orbitals of CO. The unpaired electron is in the sp_σ orbital of the metal atom pointing away from the ligand.

It has been shown that otherwise unstable carbonyls of group 11 metal atoms could be generated by cocondensation of the metal atoms and CO molecules in rare gas matrices at cryogenic temperature (4–20 K).[1-4] The thorough analyses of the vibrational spectra of the resulting matrices by Ozin et al. clearly established the formation of $Cu(CO)_n$ (n = 1, 2, 3),[2] $Ag(CO)_n$ (n = 1, 2, 3),[3] and $Au(CO)_n$ (n = 1, 2)[4] in the respective systems. They also showed that the mono- and dicarbonyl species were linear, while the tricarbonyls were trigonal planar.

Recently we have reported on the ESR (electron spin resonance) spectra of Cu(CO) and $Cu(CO)_3$ and of Ag(CO) and $Ag(CO)_3$ generated in argon matrices.[5,6] The ESR spectra showed that the semifilled orbital of Cu(CO) is an sp_σ hybrid orbital of the Cu atom pointing away from the ligand, while the semifilled orbitals of $Cu(CO)_3$ and $Ag(CO)_3$ represent the back-donation from the valence p_π orbital of the metal atom into the antibonding π^* orbitals of the CO moiety. In contrast, the ESR spectrum of Ag(CO) was essentially that of slightly perturbed Ag atoms; the magnitude of the observed ^{13}C hf (hyperfine) interaction was that expected from a CO molecule separated by the nearest neighbor distance of the host lattice. The dicarbonyls of these atoms with a linear structure would have a $^2\Pi$ ground state; their ESR spectra would hence be broadened beyond detection.

Reported below is an account of the ESR spectra observed when the Au atoms and CO molecules were cocondensed in argon matrices. Unlike the situations encountered in the Cu and Ag cases, only the signals of the monocarbonyl, Au(CO), were observed in addition to those of isolated metal atoms. The result is consistent with the conclusion reached earlier that $Au(CO)_3$ is not formed.[4] The spectral analysis revealed that Au(CO) is a bona fide complex with a bonding scheme similar to that of Cu(CO). The semifilled orbital is hence the sp_σ hybrid orbital of the Au atom pointing away from CO. The observed spectra also showed effects of the Au nuclear quadrupole interaction; the effects were demonstrated and the Au nuclear quadrupole coupling tensor was determined.

Table I. Observed and Computed Resonance Positions of Au(CO) in Argon Matrix[a]

	hyperfine component (m_I)			
signals	+3/2	+1/2	−1/2	−3/2
$H_\parallel$ (obsd)	2369	2889	3520	4271
$H_\parallel$ (com)	2369	2888	3521	4271
$H_\perp$ (obsd)	2478	2991	3637	4395
$H_\perp$ (com)	2478	2990	3636	4395

[a] Given in G, accuracy ±1 G, and microwave frequency = 9.425 GHz.

Experimental Section

A liquid helium cryostat system that would enable trapping of vaporized metal atoms in an inert gas matrix and examination of the resulting matrix by ESR has been described earlier.[7a] In the present series of experiments, gold atoms were generated from a resistively heated (~1500 °C) tantalum cell and were trapped in rare gas matrices containing controlled amounts of carbon monoxide (1–30%). Because of the wetting and alloying properties of molten gold, gold pellets were first placed in an alumina tube, capped with a molybdenum plug, and then placed in the tantalum cell. The gold atoms effused through an opening drilled through the Ta and alumina walls. From the line width of the ESR signals of the Au atoms, the Au atom concentration was estimated to be ~0.1%.[7b]

The ESR spectrometer used was an IBM Model ER200D. A low frequency field modulation (375 Hz) was used for the signal detection. All the spectra were obtained while the matrix was maintained at ~4 K. The spectrometer frequency locked to the sample cavity was 9.426 GHz, and the microwave power typically employed was ~20 μW. For photoirradiation of the matrix, a high-pressure xenon-arc lamp (Oriel, 1 kW unit) was used with a set of sharp cutoff filters.

(1) Ogden, J. S. *J. Chem. Soc., Chem. Commun.* **1971**, 978.
(2) Huber, H.; Künding, E. P.; Moskovits, K.; Ozin, G. A. *J. Am. Chem. Soc.* **1975**, *97*, 2097.
(3) McIntosh, D.; Ozin, G. A. *J. Am. Chem. Soc.* **1976**, *98*, 3167.
(4) McIntosh, D.; Ozin, G. A. *Inorg. Chem.* **1977**, *16*, 51.
(5) Kasai, P. H.; Jones, P. M. *J. Am. Chem. Soc.* **1985**, *107*, 813.
(6) Kasai, P. H.; Jones, P. M. *J. Phys. Chem.* **1985**, *89*, 1147.
(7) (a) Kasai, P. H. *Acc. Chem. Res.* **1971**, *4*, 329. (b) Kittel, C.; Abraham, E. *Phys. Rev.* **1953**, *90*, 238.

0002-7863/85/1507-6385$01.50/0